7-hydroxymethyl chlorophyll *a* reductase functions in metabolic channeling of chlorophyll breakdown intermediates during leaf senescence

Yasuhito Sakuraba [a,1], Ye-Sol Kim [a,1], Soo-Cheul Yoo [a], Stefan Hörtensteiner [b], Nam-Chon Paek [a,*]

[a] Department of Plant Science, Plant Genomics and Breeding Institute, and Research Institute for Agriculture and Life Science, Seoul National University, Seoul 151-921, Korea

[b] Institute of Plant Biology, University of Zurich, CH-8008 Zurich, Switzerland

* Correspondence author. Tel.: +82 2 880 4543, Fax: +82 2 877 4550.
E-mail address: ncpaek@snu.ac.kr (N.-C. Paek).

[1] These authors contributed equally to this work.

ABSTRACT

During natural or dark-induced senescence, chlorophyll degradation causes leaf yellowing. Recent evidence indicates that chlorophyll catabolic enzymes (CCEs) interact with the photosynthetic apparatus; for example, five CCEs (NYC1, NOL, PPH, PAO and RCCR) interact with LHCII. STAY-GREEN (SGR) and CCEs interact with one another in senescing chloroplasts; this interaction may allow metabolic channeling of potentially phototoxic chlorophyll breakdown intermediates. 7-hydroxymethyl chlorophyll *a* reductase (HCAR) also acts as a CCE, but HCAR functions during leaf senescence remain unclear. Here we show that in Arabidopsis, *HCAR*-overexpressing plants exhibited accelerated leaf yellowing and, conversely, *hcar* mutants stayed green during dark-induced senescence. Moreover, HCAR interacted with LHCII in in vivo pull-down assays, and with SGR, NYC1, NOL and RCCR in yeast two-hybrid assays, indicating that HCAR is a component of the proposed SGR-CCE-LHCII complex, which acts in chlorophyll breakdown. Notably, *HCAR* and *NOL* are expressed throughout leaf development and are drastically down-regulated during dark-induced senescence, in contrast with *SGR*, *NYC1*, *PPH* and *PAO*, which are up-regulated during dark-induced senescence. Moreover, *HCAR* and *NOL* are highly up-regulated during greening of etiolated seedlings, strongly suggesting a major role for NOL and HCAR in the chlorophyll cycle during vegetative stages, possibly in chlorophyll turnover.

Keywords:
chlorophyll degradation, STAY-GREEN, chlorophyll catabolic enzymes, 7-hydroxymethyl chlorophyll *a* reductase, SGR-CCE-LHCII complex

Abbreviations:

CBB, Coomassie Brilliant Blue; Chl, chlorophyll; CCE, chlorophyll catabolic enzyme; DDI, days of dark incubation; GFP, green fluorescent protein; HMChl *a*, 7-hydroxymethyl chlorophyll *a*; LHCI, light-harvesting complex I; LHCII, light-harvesting complex II; NYC1, NON-YELLOW COLORING 1 (TAIR: AT4G13250); NOL, NYC1-LIKE (AT5G04900); HCAR, 7-hydroxymethyl chlorophyll *a* reductase (AT1G04620); MCS, metal-chelating substance; PPH, pheophytinase (AT5G13800); PAO, pheophorbide *a* oxygenase (AT3G44880); RCCR, red chlorophyll catabolite reductase (AT4G37000); SGR, STAY-GREEN (AT4G22920); WAG, weeks after germination.

1. Introduction

During senescence, loss of green leaf color is caused by chlorophyll (Chl) degradation, a process in which Chl is converted to a primary fluorescent Chl catabolite (*p*FCC) through irreversible, consecutive reactions in chloroplasts. Chl catabolism requires six known Chl catabolic enzymes (CCEs) and a chloroplast metal-chelating substance (MCS) [1].

Many CCEs have been characterized. For example, two Chl *b* reductases, which convert Chl *b* to 7-hydroxymethyl Chl *a* (HMChl *a*), were identified as *NON-YELLOW COLORING 1* (*NYC1*) and *NYC1-LIKE* (*NOL*) [2,3]. During natural or dark-induced senescence, the rice and Arabidopsis *nyc1* mutants show a stay-green phenotype with dominant retention of Chl *b*. *NYC1* function is also important for seed maturation and longevity, as it degrades Chl *b* in developing seeds [4]. *NOL* was identified as an ortholog of *NYC1* in rice and the *nol* mutant phenotype strongly resembles the *nyc1* mutant phenotype [5]. However, the Arabidopsis *nol* mutants do not exhibit a stay-green phenotype [3], indicating that NOL is not essential for Chl breakdown in Arabidopsis despite its similarity to NYC1 [5]. 7-hydroxymethyl Chl *a* reductase (HCAR), which converts HMChl *a* to Chl *a*, was recently identified in Arabidopsis [6] as a homolog of cyanobacterial divinyl reductases involved in Chl biosynthesis [7]. Arabidopsis *hcar* mutants exhibit a stay-green phenotype during dark-induced senescence. It is assumed that the central Mg^{2+} ion in Chl *a* is removed by a metal-chelating substance (MCS) for the conversion to pheophytin *a*, although the MCS has not been molecularly identified to date. Pheophytinase (PPH), catalyzing the dephytylation of pheophytin *a* to pheophorbide *a*, was identified by bioinformatic tools in Arabidopsis [8] and by map-based cloning in a stay-green *nyc3* mutant in rice [9]. Next, pheophorbide *a* is converted to red Chl catabolite (RCC) by pheophorbide *a* oxygenase (PAO). Interestingly, pheophorbide *a* accumulates to high levels in the *hcar* mutant during dark-induced senescence although the PAO levels in *hcar* are almost identical to wild type, suggesting that high levels of HMChl *a* in *hcar* inhibit PAO function [6]. Finally, RCC is reduced to non-phototoxic *p*FCC by RCC reductase (RCCR) [10]. The Arabidopsis *pao* and *rccr* mutants were originally isolated as *accelerated cell death1* (*acd1*) and *acd2* mutants, respectively [11,12]. PAO-deficient *pao*/*acd1* and RCCR-deficient *acd2* mutants exhibit severe leaf necrosis phenotypes because of

excessive accumulation of phototoxic pheophorbide *a* and RCC, respectively [10,13]. These severe cell-death phenotypes imply that a finely tuned regulation mechanism exists in wild type to avoid the accumulation of phototoxic Chl breakdown intermediates during Chl degradation.

STAY-GREEN (*SGR*), Mendel's green cotyledon gene, encodes a novel chloroplast protein, and *SGR* orthologs have been isolated as stay-green mutants in several plant species [14-18]. Although SGR is not a CCE, it is considered to be a key regulator of LHCII destabilization because *SGR* overexpression activates premature Chl degradation in developing leaves by interacting with LHCII [14]. Recently, we showed that five CCEs (NYC1, NOL, PPH, PAO and RCCR) also interact with LHCII in vivo [19]. In addition, SGR and CCEs interact directly or indirectly with one another in vitro and in vivo, suggesting that SGR and CCEs form a dynamic multiprotein complex at LHCII (termed SGR-CCE-LHCII complex) in senescing chloroplasts to minimize the risk of photodynamism of Chl breakdown intermediates during natural or dark-induced senescence.

As described above, the enzymatic function of HCAR has been well characterized [6], but its developmental functions and its relationship with SGR or other CCEs have not been examined. Here we examine these functions and show that in Arabidopsis, *HCAR*-overexpressing plants have accelerated leaf yellowing in during dark-induced senescence. We also examine the interactions between HCAR and other CCES, finding that HCAR interacts with LHCII subunits. Furthermore, HCAR also interacts with SGR, NYC1, NOL and RCCR in yeast two-hybrid assays, indicating that HCAR functions in Chl degradation as a component of the SGR-CCE-LHCII complex during leaf senescence. A possible major role for HCAR and NOL in the Chl cycle during vegetative stages, and possibly in Chl turnover, is discussed.

2. Materials and methods

2.1. Plant materials & growth conditions

The T-DNA insertion *hcar* mutant (SALK_018790C) was obtained from the Arabidopsis Biological Resource Center (ABRC, USA). Wild type (Col-0), *hcar* mutants, and transgenic Arabidopsis plants (see below) were grown on soil in a growth

chamber at 22°C under cool-white fluorescent light (90 μmol m^{-2} s^{-1}) under long-day (16 h light/8 h dark) conditions. For dark treatment, 3-week-old plants were transferred to complete darkness. After dark incubation, the rosette leaves were sampled under weak green light. For the greening experiment, Arabidopsis seeds were germinated and the plants were grown on phytoagar plates (0.8% [w/ v]) containing 0.5X Murashige-Skoog medium at 22°C in darkness for 3 d. The etiolated seedlings were then transferred to light (90 μmol m^{-2} s^{-1}) for 12 h for greening.

2.2. Plasmid construction and Arabidopsis transformation

The Arabidopsis full-length *HCAR* cDNA without the stop codon was amplified by RT-PCR. After insertion into the Gateway entry vector pCR8/GW/TOPO (Invitrogen), the insertion was recombined into the binary Gateway vector pEarleyGate 103 [20] to introduce a C-terminal GFP tag (*35S:HCAR-GFP*). The primers used for cloning are listed in Supplementary Table 1. Arabidopsis transformation was performed as previously described [19]. The negative control (*35S:GFP*) was described previously [19].

2.3. Pigment analysis

Chl was extracted from rosette leaves with ice-cold acetone. Extracts were centrifuged at 15,000 rpm for 10 min at 4°C. The supernatant was diluted with ice-cold water to a final acetone concentration of 80% (v/v). Chl concentration was quantified as previously described [21].

2.4. SDS-PAGE and immunoblot analysis

Membrane-enriched and soluble protein fractions were extracted from the rosette leaves of transgenic Arabidopsis plants using the Native Membrane Protein Extraction Kit (Calbiochem). Protein fractions were suspended with an equal volume of 2X sample buffer (50 mM Tris, pH 6.8, 2 mM EDTA, 10% [w/v] glycerol, 2% [w/v] SDS, and 6% [v/v] 2-mercaptoethanol) and subjected to SDS-PAGE. For visualization of protein bands, polyacrylamide gels were stained with Coomassie Brilliant Blue (CBB;

Sigma-Aldrich). The resolved proteins were electro-blotted onto Immobilon-P Transfer Membrane (Millipore). Antibodies against GFP (Abcam), SGR [14], NYC1 and NOL [5], PAO (Agrisera, Sweden), RCCR [10] and photosystem proteins (Agrisera, Sweden) were used for immunoblot analysis with the WESTSAVE chemiluminescence detection kit (AbFrontier, Korea).

2.5. In vivo pull-down assays

Three-week-old transgenic plants containing the *35S:HCAR-GFP* or *35S:GFP* (negative control) were homogenized with the Native Membrane Protein Extraction Kit (Calbiochem), and the membrane-enriched fractions were pulled down using anti-GFP-conjugated agarose beads (MBL, Japan). The beads were washed at least three times with washing buffer (50 mM Tris [pH 7.2], 200 mM NaCl, 0.1% [v/v] Nonidet P-40, 2 mM EDTA, and 10% [v/v] glycerol). Washed beads were boiled with 20 μL of 2X SDS sample buffer for 5 min and the supernatants were subjected to SDS-PAGE for immunoblot analysis.

2.6. Yeast two-hybrid assays

The full-length *HCAR* cDNA in the entry vector pCR8/GW/TOPO was inserted into the destination vector pDEST32 (bait) (Invitrogen). Prey vectors for *SGR* and five *CCEs* were previously prepared in pDEST22 [19]. The yeast strain MaV203 was used for co-transformation of bait and prey clones, and β-galactosidase activity was measured by a liquid assay using chlorophenol red- β-D-galactoside (CPRG; Roche Applied Science) according to the Yeast Protocol Handbook (Clontech).

2.7. Gene expression analysis by qRT-PCR

Total RNA was extracted from rosette leaves with the Total RNA Extraction Kit including RNase-free DNase (iNtRON Biotechnology, Korea). First-strand cDNAs were synthesized with 5 μg total RNA using M-MLV reverse transcriptase and oligo(dT)15 primer in a 20 μL reaction, according to the manufacturer's instructions (Promega). Then, each 20 μL reaction was diluted to 100 μL with water and the

first-strand cDNAs were used for quantitative real-time PCR (qRT-PCR) analysis. The qRT-PCR mixture (20 μL) contained 2 μL first-strand cDNA template, 10 μL LightCycler 480 SYBR Green I Master (Roche), and 0.25 μM gene-specific forward and reverse primers (see Supplemental Table 1). PCR was performed using the Light Cycler 2.0 instrument (Roche Diagnostics). The transcript levels of each gene were normalized against those of *GAPDH* (glyceraldehyde phosphate dehydrogenase, At1g16300) as previously reported [19, 22].

3. Results

3.1. HCAR interacts with LHCII, SGR and CCEs

Recent results suggest that Chl degradation during leaf senescence involves dynamic interactions of multiple proteins, including LHCII, but not LHCI. For example we showed that SGR and five CCEs (NYC1, NOL, PPH, PAO and RCCR) interact directly or indirectly with each other in vivo and in vitro [19]. In vivo pull-down assays revealed that SGR and the CCEs interact with LHCII. Because HCAR was recently identified as a CCE involved in Chl *b* to Chl *a* reduction [6], we investigated whether HCAR also participates in Chl degradation in senescing leaves as a component of the SGR-CCE-LHCII complex [19].

To test this possibility, we first looked for proteins that interacted with HCAR. To this end, we produced transgenic Arabidopsis plants containing *35S:HCAR-GFP* (see Methods) for in vivo pull-down assays. The expression levels of *HCAR-GFP* in independent transgenic lines were evaluated by qRT-PCR and the line showing the highest expression (hereafter termed *HCAR*-OX) was selected for further experiments (Fig. 1A). Similar to the phenotypes of plants overexpressing any of the other five *CCEs* [19], *HCAR*-OX exhibited accelerated leaf yellowing during dark-induced senescence, in contrast with the stay-green phenotype of the *hcar* mutant (Fig. 1B) [6]. To quantify these phenotypes, we further determined the levels of Chl and photosystem proteins in the leaves of *HCAR*-OX and *hcar* plants (Fig. 1C and 1D). Before dark treatment (0 DDI; day of dark incubation), the levels of Chl and photosystem proteins in *HCAR*-OX and *hcar* were almost the same as those of wild type, indicating that the modulation of *HCAR* expression does not affect Chl metabolism during the vegetative

stage. During dark-induced senescence, however, Chl levels of *HCAR*-OX decreased significantly faster than in wild type, and Chl was retained in *hcar* (Fig. 1C). Similarly, photosystem proteins also showed altered stabilities in *HCAR*-OX and *hcar* plants (Fig. 1D). These results indicated that mRNA abundance of *HCAR* is directly proportional to degradation rates of Chl and photosystem proteins in senescing leaves, similar to the other *CCEs* [19].

To further examine its potential interactions, we examined the subcellular localization of the GFP-fused HCAR. As expected for a CCE, HCAR-GFP localized in the chloroplasts of *HCAR*-OX plants (Fig. S1A) and was mainly present in the membrane-enriched fractions of total protein extracts (Fig. S1B). We next used this information to enrich for interacting proteins. Using the membrane-enriched fractions of dark-incubated *HCAR*-OX plants (2 DDI) for pull-down experiments with anti-GFP agarose beads, we found that HCAR interacts with LHCII subunits (Lhcb1, 2, 4, and 5) and weakly with Lhca2 (Fig. 2A), but not with other photosystem proteins. We next examined whether HCAR co-immunoprecipitated with SGR and four CCEs by using antibodies against SGR, NYC1, NOL, PAO and RCCR (anti-PPH antibody is currently unavailable). These results revealed that native SGR and all tested CCEs co-immunoprecipitated with HCAR-GFP (Fig. 2B). To support the co-immunoprecipitation experiments, we further used yeast two-hybrid assays to examine the pairwise interaction of HCAR with SGR and five CCEs (NYC1, NOL, PPH, PAO, and RCCR) (Fig. 2C). These analyses confirmed the interactions of HCAR with SGR, NYC1, NOL and RCCR. Together, these results demonstrate that HCAR is a component of the SGR-CCE-LHCII complex in senescing chloroplasts.

3.2. Expression patterns of SGR and 6 CCEs during leaf development

To determine whether SGR and the CCEs also act in Chl metabolism, i.e. Chl turnover, in addition to their involvement in senescence-related Chl degradation [23], we examined their expression in pre-senescent stages and in dark-induced senescence. We compared their expression profiles in whole rosettes of wild type plants up to 6 weeks after germination (6 WAG) under long-day conditions (Fig. S2), with leaves of 3-week-old plants during dark-induced senescence (Fig. S3). Expression of *SGR*, *NYC1*, *PPH* and *PAO* was highly induced during natural senescence (5-6 WAG) (Fig. S2A-D)

and during dark-induced senescence (Fig. S3A-D). By contrast, *HCAR*, *NOL* and *RCCR* were constantly expressed throughout development (Fig. S2E-G), and two CCEs, *NOL* and *HCAR*, were drastically down-regulated during dark-induced senescence (Fig. S3E and S3F).

Chl turnover rates are especially high during greening of etiolated seedlings [23]. Therefore, we further examined *SGR* and *CCE* expression during greening of etiolated seedling and compared with 4-week-old mature leaves before dark incubation (4W) or after 3 DDI (4WD) (Fig. 3). When the 3-d-old etiolated seedlings were exposed to white light (90 μmol m^{-2} s^{-1}) for 12 h, we found that the low mRNA levels of *SGR*, *NYC1*, *PPH* and *PAO* in etiolated seedlings were not significantly changed by exposure to 12h of light (Fig. 3A-D) and gene expression was up-regulated only during dark-induced senescence (4WD). By contrast, *NOL* and *HCAR* expression in seedlings increased by about 12.5- and 7.5-fold, respectively, after transfer to light. This expression was maintained at high levels during the vegetative stage, but was rapidly down-regulated during dark-induced senescence (Fig. 3E and 3F). Compared with the other five CCEs, *RCCR* expression showed less-pronounced changes in developing or senescing leaves. These results suggest that *NOL* and *HCAR* might play an important role in the Chl cycle during vegetative stages.

4. Discussion

Chl breakdown is an integral process in plant development, but as a detoxification rather than a remobilization process. For example, during vegetative growth *acd1/pao* and *acd2/rccr* mutants exhibit an accelerated cell death phenotype caused by accumulation of singlet oxygen generated from the phototoxic Chl breakdown intermediates, pheophorbide *a* and RCC, respectively [10,13,24-26]. Here we show that HCAR is an essential enzyme for Chl degradation, in addition to SGR and five CCEs (NOL, NYC1, PPH, PAO and RCCR) [19]. *HCAR*-OX accelerates Chl degradation and *hcar* mutant stays green during dark-induced senescence (Fig. 1). In vivo pull-down and yeast two-hybrid assays (Fig. 2) strongly support the hypothesis that HCAR is a component of the SGR-CCE-LHCII complex for Chl degradation in senescing leaves.

In this study, we found that expression levels of *NOL*, *HCAR* and *RCCR* are relatively constant throughout development (Fig. S2). RCCR localizes in both

chloroplasts and mitochondria in seedling leaves [25]. In mitochondria, RCCR plays an important role in protecting cells from programmed cell death (PCD) that involves an early mitochondrial oxidative burst. In addition, RCCR localizes to chloroplasts, mitochondria and cytosol under bacterial infection. This supports the hypothesis that Chl intermediates modulate PCD under biotic stress conditions [26]. By contrast, NOL and HCAR are exclusively localized in chloroplasts [5, 6] and highly expressed in non-senescent leaves (Figs. 3, S2 and S3). Based on our previous [19] and present results, the interactions among CCEs can be divided into two groups according to their expression patterns. Although SGR and RCCR interact with each other and with the other five CCEs in senescing chloroplasts, the pairwise interactions among the CCEs are more selective, i.e., PPH-PAO and NYC1-NOL-HCAR. Furthermore, expression patterns of *NOL* and *HCAR* differ from those of *NYC1*, *PPH* and *PAO* during greening of etiolated seedlings; *NOL* and *HCAR* expression is highly up-regulated in greening seedlings (EL) (Fig. 3) and is much higher than in senescing leaves (Fig. S2). These results support the idea of a major role for *NOL* and *HCAR* during vegetative stages of leaf development, including seedling development. By contrast, *SGR*, *NYC1*and *PPH* may not be critical for Chl metabolism during vegetative development.

NYC1, NOL and HCAR are responsible for the two consecutive steps from Chl *b* via HMChl *a* to Chl *a* in the Chl cycle. These steps are involved in the adaptation of the photosynthetic machinery to changing light conditions, acting to adjust Chl *a* and Chl *b* abundances [27,28]. In addition, the reductive half of the Chl cycle is also involved in Chl breakdown [3,5,6,24]. These differences in gene expression patterns indicate that NOL and HCAR might have different developmental roles than NYC1, which is primarily required during senescence. In green leaves, Chl is thought to be turned over continuously alongside with photosystem complexes, in particular the core complex components of photosystem II, which undergo a continuous repair cycle [29]. However, the extent and molecular mechanism of this Chl turnover [23] remain largely unknown. It was proposed that Chl turnover in *Synechocystis* mainly involves de- and re-phytylation steps but no further degradation [30]. In higher plants, the fate of turned-over Chl remains elusive [29], but according to the gene expression data shown here, an involvement of the CCEs that convert Chl to *p*FCC, i.e. PPH, PAO and RCCR, can be ruled out. However, NOL and HCAR might act in Chl turnover at pre-senescent stages.

It has been reported that SGR/CCEs do not interact with LHCI, as tested by immunoblotting with an anti-Lhca1 antibody [14,19]; therefore, the mechanisms of Chl degradation in LHCI during senescence have remained elusive. In this study, we found that HCAR interacts weakly with Lhca2 of LHCI in vivo (Fig. 2A). This might explain the retention of LHCI subunits in *hcar* mutants during dark-induced senescence (Fig. 1D) and might suggest the possibility that the SGR-CCE complex is also involved in the breakdown of LHCI-located Chl. The discrepancy between the previous [19] and the present results may be due a much weaker affinity of SGR and the CCEs to LHCI subunits compared to LHCII subunits. Thus, further investigation is necessary to elucidate the extent of the interaction of SGR and the CCEs with LHCI subunits. Furthermore, additional identification of complex components in non-senescent and senescing chloroplasts will provide more insights into dynamic Chl metabolism.

Acknowledgments

We thank Do-In Kim for her excellent technical support, Dr. Ayumi Tanaka for providing antibodies against NYC1 and NOL. This work was supported by grants from the Next-Generation BioGreen 21 Program (No. PJ009018), Rural Development Administration, Republic of Korea (to N.-C.P.) and the Swiss National Science Foundation (to S.H).

References

[1] S. Hörtensteiner, B. Kräutler, Chlorophyll breakdown in higher plants, Biochim. Biophys. Acta. 1807 (2011) 977-988.

[2] M. Kusaba, H. Ito, R. Morita, et al., Rice NON-YELLOW COLORING1 is involved in light-harvesting complex II and grana degradation during leaf senescence, Plant Cell 19 (2007) 1362-1375.

[3] Y. Horie, H. Ito, M. Kusaba, et al., Participation of chlorophyll *b* reductase in the initial step of the degradation of light-harvesting chlorophyll *a/b*-protein complexes in *Arabidopsis*, J. Biol. Chem. 284 (2009) 17449-17456.

[4] S. Nakajima, H. Ito, R. Tanaka, et al., Chlorophyll *b* reductase plays an essential role in maturation and storability of Arabidopsis seeds, Plant Physiol. 160 (2012) 261-273.

[5] Y. Sato, R. Morita, S. Katsuma, et al., Two short-chain dehydrogenase/reductases, NON-YELLOW COLORING 1 and NYC1-LIKE, are required for chlorophyll *b* and light-harvesting complex II degradation during senescence in rice, Plant J. 57 (2009) 120-131.

[6] M. Meguro, H. Ito, A. Takabayashi, et al., Identification of the 7-hydroxymethyl chlorophyll *a* reductase of the chlorophyll cycle in *Arabidopsis*, Plant Cell 23 (2011) 3442-3453.

[7] H. Ito, M. Yokono, R. Tanaka, et al., Identification of a novel vinyl reductase gene essential for the biosynthesis of monovinyl chlorophyll in *Synechocystis* sp. PCC6803, J. Biol. Chem. 283 (2008) 9002-9011.

[8] S. Schelbert, S. Aubry, B. Burla, et al., Pheophytin pheophorbide hydrolase (pheophytinase) is involved in chlorophyll breakdown during leaf senescence in *Arabidopsis*, Plant Cell 21 (2009) 767-785.

[9] R. Morita, Y. Sato, Y. Masuda, et al., Defect in non-yellow coloring 3, an α/β hydrolase-fold family protein, causes a stay-green phenotype during leaf senescence in rice, Plant J. 59 (2009) 940-952.

[10] A. Pružinská, I. Anders, S. Aubry, et al., In vivo participation of red chlorophyll catabolite reductase in chlorophyll breakdown, Plant Cell 19 (2007) 369-387.

[11] J.T. Greenberg, F.M. Ausubel, *Arabidopsis* mutants compromised for the control of cellular damage during pathogenesis and aging, Plant J. 4 (1993) 327-341.

[12] J.T. Greenberg, A. Guo, D.F. Klessig, et al., Programmed cell death in plants: a pathogen-triggered response activated coordinately with multiple defense functions, Cell 77 (1994) 551-563.

[13] M. Hirashima, R. Tanaka, A. Tanaka, Light-independent cell death induced by accumulation of pheophorbide *a* in *Arabidopsis thaliana*, Plant Cell Physiol. 50 (2009) 719-729.

[14] S.-Y.Park, J.W. Yu, J.-S. Park, et al., The senescence-induced staygreen protein regulates chlorophyll degradation. Plant Cell 19 (2007) 1649-1664.

[15] G. Ren, K. An, Y. Liao, et al., Identification of a novel chloroplast protein AtNYE1 regulating chlorophyll degradation during leaf senescence in *Arabidopsis*, Plant Physiol. 144 (2007) 1429-1441.

[16] Y. Sato, R. Morita, M. Nishimura, et al., Mendel's green cotyledon gene encodes a positive regulator of the chlorophyll-degrading pathway, Proc.Natl. Acad. Sci. USA 104 (2007) 14169.

[17] C.S. Barry, R.P. McQuinn, M.Y. Chung et al., Amino acid substitutions in homologs of the STAY-GREEN protein are responsible for the *green-flesh* and *chlorophyll retainer* mutations of tomato and pepper, Plant Physiol. 147 (2008) 179-187.

[18] S. Aubry, J. Mani, S. Hörtensteiner, Stay-green protein, defective in Mendel's green cotyledon mutant, acts independent and upstream of pheophorbide a oxygenase in the chlorophyll catabolic pathway, Plant Mol. Biol. 67 (2008) 243-256.

[19] Y. Sakuraba, S. Schelbert, S.-Y. Park, et al., STAY-GREEN and chlorophyll catabolic enzymes interact at light-harvesting complex II for chlorophyll detoxification during leaf senescence in *Arabidopsis*, Plant Cell (2012) 507-518.

[20] K.W. Earley, J.R. Haag, O. Pontes, et al., Gateway-compatible vectors for plant functional genomics and proteomics, Plant J. 45 (2006) 616-629.

[21] R. Porra, W. Thompson, P. Kriedemann, Determination of accurate extinction coefficients and simultaneous equations for assaying chlorophylls *a* and *b* extracted with four different solvents: verification of the concentration of chlorophyll standards by atomic absorption spectroscopy, Biochim. Biophys. Acta. 975 (1989) 384-394.

[22] Y. Sakuraba, M. Yokono, S. Akimoto, et al., Deregulated chlorophyll *b* synthesis reduces the energy transfer rate between photosynthetic pigments and induces

photodamage in *Arabidopsis thaliana*, Plant Cell Physiol. 51 (2010) 1055-1065.

[23] P. Matile, S. Hortensteiner, H. Thomas. Chlorophyll degradation, Annu. Rev. Plant Physiol. Plant Mol. Biol. 50 (1999) 67-95.

[24] S. Hörtensteiner, Chlorophyll degradation during senescence, Annu. Rev. Plant Biol. 57 (2006) 55-77.

[25] N. Yao, J.T. Greenberg. *Arabidopsis* ACCELERATED CELL DEATH2 modulates programmed cell death, Plant Cell 18 (2006) 397-411.

[26] J.M. Mach, A.R. Castillo, R. Hoogstraten, et al., The *Arabidopsis*-accelerated cell death gene *ACD2* encodes red chlorophyll catabolite reductase and suppresses the spread of disease symptoms, Proc. Natl. Acad. Sci. USA 98 (2001) 771–776.

[27] R. Tanaka, H. Ito, A. Tanaka, Regulation and functions of the chlorophyll cycle, in: C.A. Rebeiz, C. Benning, H.J. Bohnert, H. et al. (Eds.), Chloroplast: Basics and Applications, Advances in Photosynthesis and Respiration, Vol. 31, Springer, 2010, pp. 55-77.

[28] R. Tanaka, A. Tanaka, Chlorophyll cycle regulates the construction and destruction of the light-harvesting complexes, Biochem. Biophys. Acta 1807 (2011) 968-976.

[29] K.G. Beisel, S. Jahnke, D. Hofmann, et al., Continuous turnover of carotenes and chlorophyll *a* in mature leaves of Arabidopsis revealed by $^{14}CO_2$ pulse-chase labeling, Plant Physiol. 152 (2010) 2188-2199.

[30] D. Vavillin, W. Vermaas, Continuous chlorophyll degradation accompanied by chlorophyllide and phytol reutilization for chlorophyll synthesis in *Synechocystis* sp. PCC 6803, Biochim. Biophys. Acta 1767 (2007) 920-929

Figure legends

Fig. 1. Phenotypic and molecular characterization of *HCAR*-OX and *hcar* plants during dark-induced senescence.

(A) Expression levels of *HCAR-GFP* in the rosette leaves of 3-week-old *HCAR*-OX transgenic plants (OX) were measured by qRT-PCR and normalized to the internal control gene *GAPDH* (glyceraldehyde phosphate dehydrogenase, At1g16300). Expression levels were compared with those of wild type (WT) control, which was set as 1 (see Methods). The OX-3 plants showed the highest expression of *HCAR-GFP*, about 10-fold higher than wild type. Means and SD values in (A, C) were obtained from five biological replicates.

(B) Visible phenotypes of 3-week-old WT, *HCAR*-OX and *hcar* plants before dark treatment (0 DDI) and after 4 DDI. Compared with WT, *HCAR*-OX exhibited accelerated leaf yellowing and *hcar* mutants stayed green. DDI, days of dark incubation.

(C, D) Changes in total Chl content (C) and photosynthetic proteins (D) in the rosette leaves of 3-week-old WT, *hcar* and *HCAR*-OX plants during dark-induced senescence. Bars indicate 0 (black), 4 (grey) and 7 DDI (white). (D) The immunoblot experiments were performed three times with similar results. Antibodies against Lhcb1, Lhca1, D1 and PsaA were used for detection.

Fig. 2. HCAR is a member of SGR-CCE-LHCII complex in senescing chloroplasts.

(A, B) Three-week-old *HCAR*-OX (*35S:HCAR-GFP*) and negative control (*35S:GFP*) plants were dark-incubated for 2 d. The HCAR-GFP and GFP was pulled down with anti-GFP-conjugated agarose beads from membrane-enriched fractions of total protein extracts from rosette leaves.

(A) HCAR interacts with LHCII in in vivo pull-down assays. Note that the interaction of HCAR with the Lhca2 subunit of LHCI was detected when the X-ray film was exposed to the immunoblotted membranes much longer (2 min) than the others (15 sec).

(B) HCAR co-immunoprecipitated with SGR and four CCEs in vivo. The presence of PPH could not be examined due to unavailability of antibodies against PPH.

(C) Interactions of HCAR with SGR and five CCEs by yeast two-hybrid assays. β-Galactosidase (β-Gal) activity was measured by a liquid assay using chlorophenol red-β-D-galactosidase (CPRG). Empty bait and prey plasmids (-) were used as negative

controls. Mean and SD values were obtained from five independent colonies. (A-C) These experiments were performed at least twice with the same results.

Fig. 3. Expression of *SGR* and *CCEs* during different stages of plant development.
Expression levels of *SGR* (A), *NYC1* (B), *PPH* (C), *PAO* (D), *NOL* (E), *HCAR* (F) and *RCCR* (G) were examined by qRT-PCR in 3-d-old etiolated seedlings before (ET) and after 12 hours of light exposure (EL; cool-white light intensity, 90 μmol m^{-2} s^{-1}). Expression levels in ET and EL are compared with those in rosette leaves of 4-week-old plants before (4W) and after 3 DDI (4WD). Relative expression levels of each gene were normalized to the mRNA levels of *GAPDH*. Expression levels for each gene are shown relative to the expression in ET, which is set as 1. Mean and SD values were obtained from more than six biological replicates.

Figure 1.

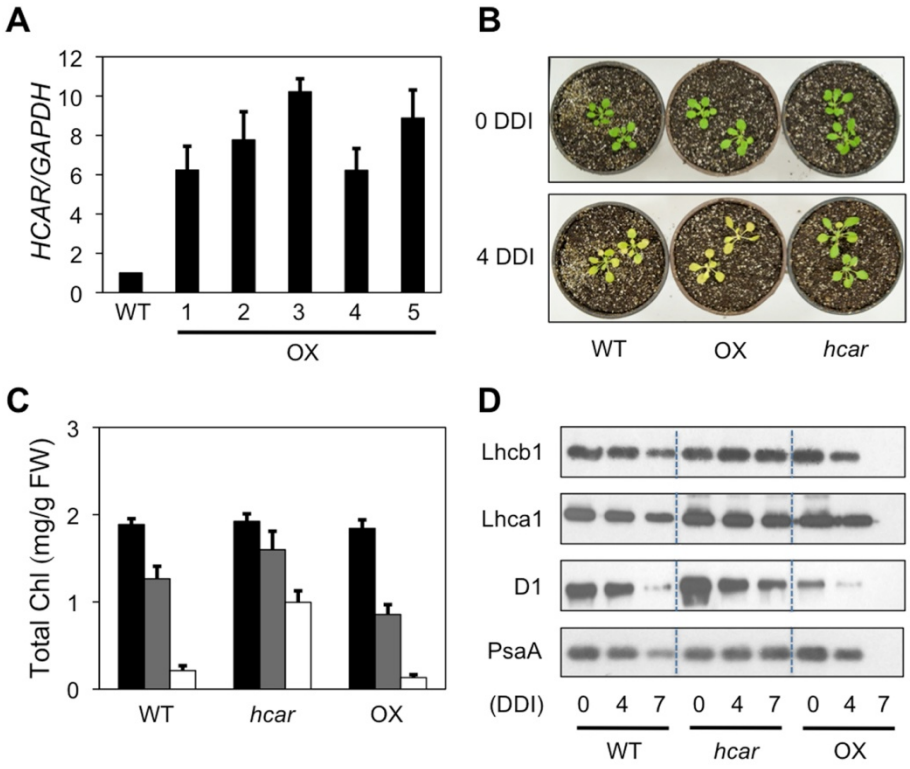
A
HCAR/GAPDH
12
10
8
6
4
2
0
WT
1
2
3
4
5
OX
B
0 DDI
4 DDI
WT
OX
hcar
C
Total Chl (mg/g FW)
3
2
1
0
WT
hcar
OX
D
Lhcb1
Lhca1
D1
PsaA
(DDI)
0 4 7 0 4 7 0 4 7
WT
hcar
OX

Figure 2.

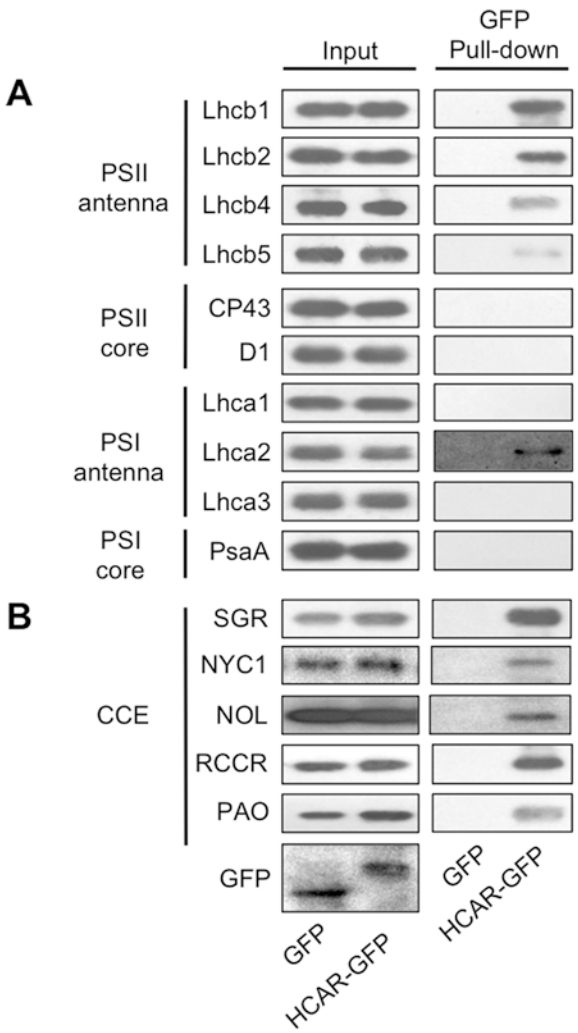
A
Input
GFP Pull-down
PSII antenna
Lhcb1
Lhcb2
Lhcb4
Lhcb5
PSII core
CP43
D1
PSI antenna
Lhca1
Lhca2
Lhca3
PSI core
PsaA
B
CCE
SGR
NYC1
NOL
RCCR
PAO
GFP
GFP
HCAR-GFP
GFP
HCAR-GFP

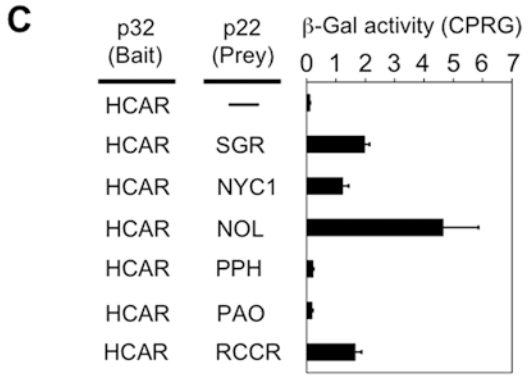
C
p32 (Bait)
p22 (Prey)
β-Gal activity (CPRG)
0 1 2 3 4 5 6 7
HCAR —
HCAR SGR
HCAR NYC1
HCAR NOL
HCAR PPH
HCAR PAO
HCAR RCCR

Figure 3.

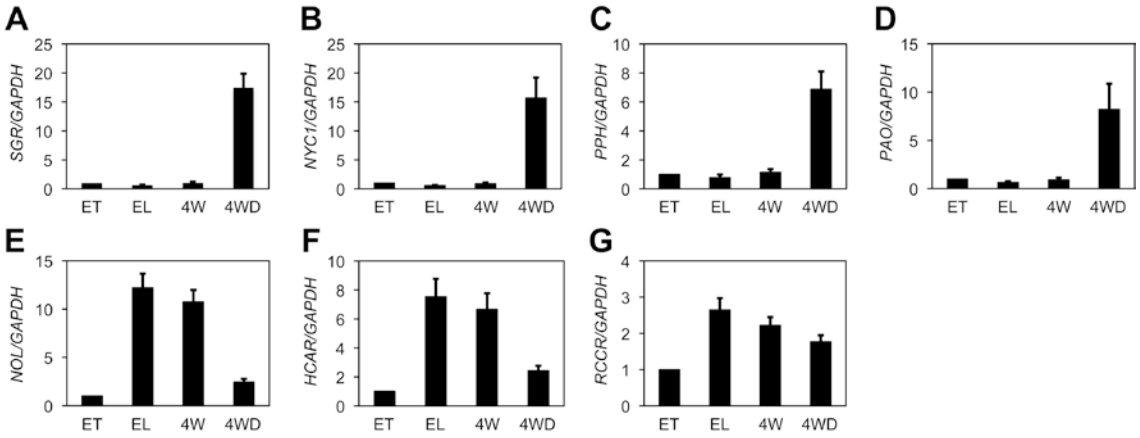
A
SGR/GAPDH
25
20
15
10
5
0
ET EL 4W 4WD
B
NYC1/GAPDH
25
20
15
10
5
0
ET EL 4W 4WD
C
PPH/GAPDH
10
8
6
4
2
0
ET EL 4W 4WD
D
PAO/GAPDH
15
10
5
0
ET EL 4W 4WD
E
NOL/GAPDH
15
10
5
0
ET EL 4W 4WD
F
HCAR/GAPDH
10
8
6
4
2
0
ET EL 4W 4WD
G
RCCR/GAPDH
4
3
2
1
0
ET EL 4W 4WD

Supplementary Materials

7-hydroxymethyl chlorophyll *a* reductase functions in metabolic channeling of chlorophyll breakdown intermediates during leaf senescence

Yasuhito Sakuraba, Ye-Sol Kim, Soo-Cheul Yoo, Stefan Hörtensteiner, Nam-Chon Paek

Supplementary Materials & Methods

1. Subcellular localization of HCAR-GFP

GFP fluorescence images were recorded with a laser scanning confocal microscope (LSM510, Carl Zeiss-LSM510). An argon laser (25 mW) was used for generating an excitation source at 488 nm. GFP and Chl fluorescence were recorded at 525 nm and 660 nm, respectively.

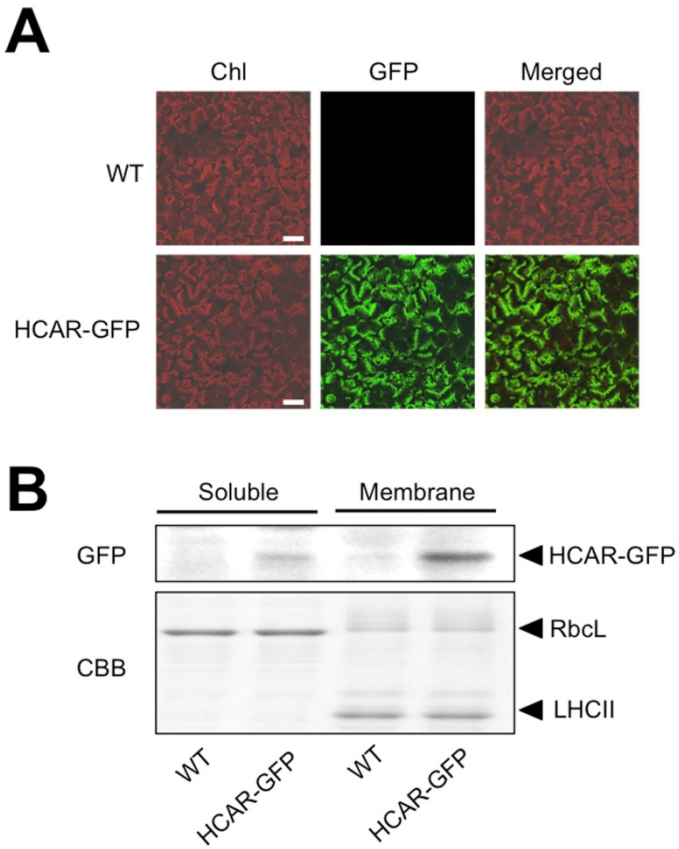

Supplementary Fig. 1. HCAR localizes in the chloroplasts and exists in the membrane factions of total protein extracts.

(A) Subcellular localization of HCAR-GFP protein observed in the rosette leaves of *HCAR*-OX plants by laser scanning confocal microscopy. Red Chl autofluorescence (left), green GFP fluorescence (middle), and merged image (right) are shown, respectively. GFP fluorescence was collected at 520 nm and Chl autofluorescence was collected at 680 nm. WT, wild type. Bars = 50 μm.

(B) HCAR-GFP is enriched in the membrane fraction in total protein extracts. Total protein extracts were obtained from the rosette leaves of 2-week-old plants of wild type (WT) and *HCAR*-OX plants (see Methods). GFP fusion proteins were detected by immunoblotting with an anti-GFP antibody (upper panel). The Coomassie Brilliant Blue (CBB)-stained polyacrylamide gel is shown as loading control (lower panel).

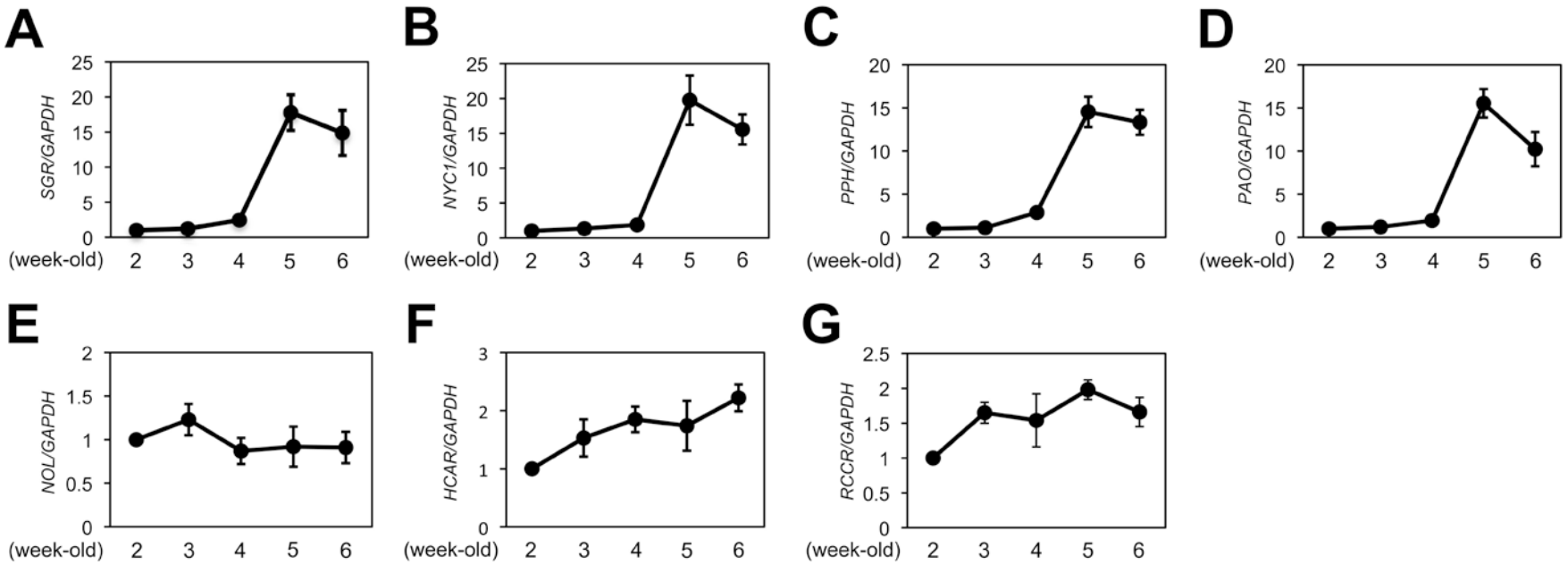

Supplementary Fig. 2. Expression patterns of *SGR* and six *CCEs* during plant development.

By using qRT-PCR analysis, changes in the expression levels of *SGR* (A), *NYC1* (B), *PPH* (C), *PAO* (D), *NOL* (E), *HCAR* (F) and *RCCR* (G) were examined in the rosette leaves of 2-, 3-, 4-, 5- and 6-week-old plants. Under the used long-day growth conditions (16-h light/8-h dark), natural senescence in Arabidopsis (Col-0) began from 4 weeks after germination (4 WAG). Expression levels of each gene were normalized to the internal control gene *GAPDH*. Expression levels for each gene are shown relative to the expression in 2-week-old plants, which is set as 1. Mean and SD values were obtained from more than six biological replicates.

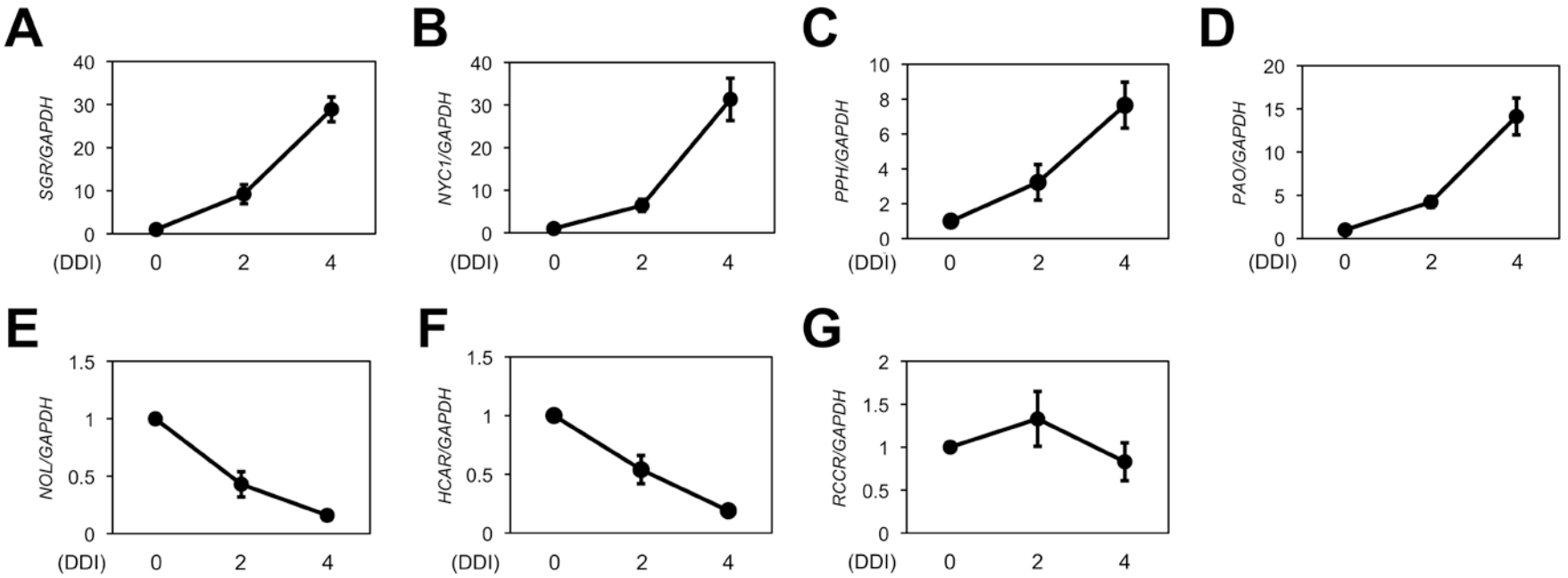

Supplementary Fig. 3. Expression patterns of *SGR* and six *CCEs* during DIS.

By using qRT-PCR analysis, changes in the expression levels of *SGR* (A), *NYC1* (B), *PPH* (C), *PAO* (D), *NOL* (E), *HCAR* (F) and *RCCR* (G) were examined in the rosette leaves of 3-week-old plants during dark-induced senescence, after 2 and 4 days of dark incubation (DDI). Expression levels of each gene were normalized to the internal control gene *GAPDH*. Expression levels for each gene are shown relative to the expression in 0-DDI plants, which is set as 1. Mean and SD values were obtained from more than six biological replicates.

Supplementary Table 1. Primers used in this study.

Gene	Forward primer (5'→3')	Reverse primer (5'→3')
Transgenic		
HCAR	ATGATTACTGTCGTCACCT	TTTCTTGGAGAGCATTTTATCTA
qRT-PCR		
SGR	GGTGGCCATTTCCTTTTAGA	TCAACAAGTTCCCATCTCCA
NYC1	TTCTCAGTGGTTCGAGCATT	AGGTAATTGACGGCTTTTCC
NOL	TGCAGATGCAAGATGTCAAA	TGGTGTAGGCTTTGATTCCA
HCAR	CGGTACTCGTTGGACTACCAT	CTATTTGGCCGTTTTTTGTTGT
PPH	TCTCACGTATTGTGGAGGTC	ATAGCTCTCCACCAGGAGCA
PAO	CTCTGGTTTGATCGGAATGAT	GAAGCTCGTGCTGTTAAATCC
RCCR	CGCCGAAAATTTATGGAGTT	AGGGAAGGAGTTGTGATTGG
GAPDH	TTGGTGACAACAGGTCAAGCA	AAACTTGTCGCTCAATGCAATC